A mitochondrial enzyme degrades carotenoids and protects against oxidative stress

Jaume Amengual,*,[1] Glenn P. Lobo,*,[1] Marcin Golczak,* Hua Nan M. Li,* Tatyana Klimova,* Charles L. Hoppel,* Adrian Wyss,† Krzysztof Palczewski,* and Johannes von Lintig*,[2]

*Department of Pharmacology, School of Medicine, Case Western Reserve University, Cleveland, Ohio, USA; and †Research and Development, Human Nutrition and Health, DSM Nutritional Products Ltd., Basel, Switzerland

ABSTRACT **Carotenoids are the precursors for vitamin A and are proposed to prevent oxidative damage to cells. Mammalian genomes encode a family of structurally related nonheme iron oxygenases that modify double bonds of these compounds by oxidative cleavage and *cis*-to-*trans* isomerization. The roles of the family members BCMO1 and RPE65 for vitamin A production and vision have been well established. Surprisingly, we found that the third family member, β,β-carotene-9′,10′-oxygenase (BCDO2), is a mitochondrial carotenoid-oxygenase with broad substrate specificity. In BCDO2-deficient mice, carotenoid homeostasis was abrogated, and carotenoids accumulated in several tissues. In hepatic mitochondria, accumulated carotenoids induced key markers of mitochondrial dysfunction, such as manganese superoxide dismutase (9-fold), and reduced rates of ADP-dependent respiration by 30%. This impairment was associated with an 8- to 9-fold induction of phosphor-MAP kinase and phosphor-AKT, markers of cell signaling pathways related to oxidative stress and disease. Administration of carotenoids to human HepG2 cells depolarized mitochondrial membranes and resulted in the production of reactive oxygen species. Thus, our studies in BCDO2-deficient mice and human cell cultures indicate that carotenoids can impair respiration and induce oxidative stress. Mammalian cells thus express a mitochondrial carotenoid-oxygenase that degrades carotenoids to protect these vital organelles.—Amengual, J., Lobo, G. P., Golczak, M., Li, H. N. M., Klimova, T., Hoppel, C. L., Wyss, A., Palczewski, K., von Lintig, J. A mitochondrial enzyme degrades carotenoids and protects against oxidative stress. *FASEB J.* 25, 948–959 (2011). www.fasebj.org**

Key Words: carotenoid-oxygenases · apocarotenoids · respiration · reactive oxygen species

Carotenoids are isoprenoid pigments with characteristic chemical structures and physical properties that are synthesized in plants, certain fungi, and bacteria. Pure hydrocarbon carotenoids, such as β,β-carotene and lycopene, are termed carotenes, whereas their oxygenated derivatives, such as zeaxanthin and lutein, are called xanthophylls. Physiological functions attributed to these compounds are associated with their capability to eliminate excess energy, act as free radical scavengers, and quench singlet oxygen in photosynthetic organisms (for review, see ref. 1). A protective role of carotenoids against oxidative stress has been also proposed for human cells. For example, the central part of the human retina, the macula lutea, owes its yellow color to high levels of the xanthophylls lutein and zeaxanthin (2, 3). These xanthophylls have been suggested to prevent light damage to the retina (4).

Carotenoids also are converted to apocarotenoids by an ancestral family of nonheme iron oxygenases that are crucial for many physiological processes in plants and animals (for review, see ref. 5). Mammalian genomes encode three different family members of these enzymes. The retinal pigment epithelium protein of 65 kDa (RPE65) was first discovered and is essential for vision (6). Biochemical analysis shows that RPE65 catalyzes a *trans*-to-*cis* isomerization of retinoids, the key step in the retinoid cycle of the eyes (for review, see ref. 7). The two other family members are real carotenoid-oxygenases that catalyze the oxidative cleavage of distinct double bonds of carotenoids and are expressed in various tissues and cell types. The β,β-carotene-15,15′-monooxygenase (BCMO1) localizes to cytoplasm and converts a limited number of carotenoids, such as β,β-carotene, to retinoids (8). Studies in knockout (KO) mice and humans show that BCMO1 is the critical enzyme for vitamin A production (9, 10). The physiological function of the β,β-carotene-9′,10′-oxygenase (BCDO2) is less well understood. Biochemical studies reveal that this enzyme cleaves carotenes such as β,β-carotene and lycopene at the C10,C9 double bond

[1] These authors contributed equally to this work.

[2] Correspondence: Department of Pharmacology (W333), School of Medicine, Case Western Reserve University, 10900 Euclid Ave., Cleveland, OH 44160, USA. E-mail: johannes.vonlintig@case.edu

doi: 10.1096/fj.10-173906

This article includes supplemental data. Please visit *http://www.fasebj.org* to obtain this information.

0892-6638/11/0025-0948 © FASEB

to yield a long-chain and a short-chain apocarotenoid (11, 12). Such eccentric cleavage of β,β-carotene has been discussed as an alternative route for vitamin A production (for review, see ref. 13). However, BCMO1 mice become vitamin A deficient despite expressing BCDO2 (9), suggesting a different physiological function of this enzyme.

A more diversified role of BCDO2 for carotenoid metabolism is indicated by recent genetic studies. In chickens, bovines, and sheep, mutations in the BCDO2 gene alter levels of β,β-carotene and xanthophylls in tissues and blood (14–17). In humans, a single-base-pair polymorphism in intron 2 of *BCDO2* gene has been identified that correlates with altered blood levels of interleukin 18, a proinflammatory cytokine associated with type 2 diabetes and cardiovascular disease (18). An association of BCDO2 and cardiovascular disease also has been found in mice (19). These findings suggest that BCDO2 not only plays a key role in carotenoid homeostasis but that genetic polymorphism in this gene can give rise to disease. Therefore, we studied the biochemical properties of this enzyme and analyzed the consequences of BCDO2 deficiency in a mouse model.

MATERIALS AND METHODS

Materials

All chemicals, unless stated otherwise, were purchased from Sigma-Aldrich (St. Louis, MO, USA). Reagents for cDNA synthesis and quantitative real-time PCR (qRT-PCR) were purchased from Applied BioSystems (Foster City, CA, USA). Primary antibodies, anti-phospho-Akt, anti-phospho-MAPK, and anti-MnSOD were obtained from Upstate Biotechnology (Waltham, MA, USA). Anti-COX IV and anti-HIF1α antibodies were obtained from Novus Biologicals (Littleton, CO, USA) and anti-RAN (protein loading control) was from Abcam (Cambridge, MA, USA). The BCDO2 polyclonal antibody was generated in mice against His-tagged recombinant human BCDO2 purified by affinity chromatography (Institut für Immunbiologie, University of Freiburg, Freiberg, Germany). Anti-mouse and anti-rabbit horseradish peroxidase-conjugated secondary antibodies were purchased from Promega (Madison, WI, USA) or Bio-Rad Laboratories (Hercules, CA, USA).

Targeting construct, electroporation of embryonic stem (ES) cells, and generation of *BCDO2*-KO (*BCDO2*$^{-/-}$) chimera

Homozygous recombination was used to obtain the *BCDO2*$^{-/-}$ mouse. Briefly, we isolated 2 clones by PCR screening of a 129SvJ mouse BAC library (Genome Systems, St. Louis, MO, USA). A fragment of the *BCDO2* gene (including exons 1 to 4 and part of exon 5) was replaced by the NLS-*lacZ* gene and a *neomycin*^{R} (*neo*^{R}) cassette without affecting the 5′ promoter region. The flanking sequences (5′ arm, 4.9-kb *Pst*I-*Nco*I fragment; 3′ arm, 4.4-kb *Sma*I-*Nco*I fragment) were cloned into pBS vector. Approximately 9.2 kb, including exons 1 to 4 and part of exon 5, was deleted from the wild-type (WT) BCDO2 allele and replaced by an NLS-*lacZ* cassette, followed by a *neo*^{R} cassette between two *lox*P sites. ES cells (from mouse strain 129SvJ/SvEvTac) were routinely cultured and subjected to G418 selection. For electroporation of cells, the targeting vector was linearized with *Not*I and 20 μg of the purified target construct was added to 0.8 ml of a single cell suspension (5×10^6 cells/ml in phosphate-buffered saline (PBS) without Ca^{2+} and Mg^{2+} (137 mM NaCl, 2.7 mM KCl, 10 mM sodium phosphate dibasic, and 2 mM potassium phosphate, pH 7.4) and placed in a GenePulser (Bio-Rad) at 240 V, 500 μF. After electroporation, cells were seeded onto neomycin-resistant embryonic fibroblasts. Selection with 200 mg/ml G418 was initiated after 48 h, and individual clones were isolated 10–12 d after electroporation. All clones were screened for homologous recombination by Southern blot analysis using two specific probes and subjected to staining for β-galactosidase activity (data not shown). A selected clone that had undergone homologous recombination was injected into blastocysts. Injected blastocysts were then transferred into pseudopregnant foster mothers. Chimerism was estimated according to the coat color of the litter. Male chimeric mice were backcrossed to C57BL6 mice to obtain heterozygous and subsequently homozygous mice.

The Easy-DNA kit (Invitrogen, Carlsbad, CA, USA) was used to isolate genomic DNA from mouse-tail biopsies. For the WT gene, PCR was performed with the following primers: BCDO2 up, 5′-ATACAATCATTGGTTTGATGGAA-3′, and BCDO2 down, 5′-TAGGTGGCTCAAACCTTGACA-3′. For the KO gene, PCRs were performed using the following primer pairs: Ko up, 5′-CAGTCACGACGTTGTAAAAC-3′, and Ko down, 5′-CTTCCTGTGGCAGTGTACCATCG-3′; lacZ reverse down, 5′-CTCGCCGCACATCTGAACTTCAG-3′, and lacZ reverse up, 5′-CTTCCTGTGGCAGTGTACCATCG-3′; lacZ forward up, 5′-AAGGTGTCATGACACATGACAG-3′, and lacZ forward down, 5′-GTTCAACATCAGCCGCTACAG-3′.

Animals and diets

Animal experiments were performed in accordance with U.S. animal protection laws in adherence with guidelines of the institutional animal care and use committee of Case Western Reserve University (Cleveland, OH, USA). Mice were kept in a room under controlled conditions (24°C, 12-h light-dark cycle) with free access to food and water. Five-week-old WT, *BCDO2*$^{+/-}$ [heterozygous (HET)] and *BCDO2*$^{-/-}$ (KO) male and female mice (n=5–10 animals/group) were maintained on standard chow diet, or vitamin A-deficient diets supplemented with 0.05 mg/g zeaxanthin (zeaxanthin diet) or 0.05 mg/g lutein (lutein diet) for 8 wk, after which they were euthanized. Vitamin A-deficient diets were based on an AIN-93G formulation and prepared by Research Diets, (New Brunswick, NJ, USA). Zeaxanthin (zeaxanthin diet) and lutein (lutein) was added in a water-soluble formulation (beadlets), provided by DSM Nutritional Products (Basel, Switzerland). Control diet was without carotenoids.

Tests for enzymatic activity and HPLC analysis of carotenoids

For tests for enzymatic activity, full-length cDNA for murine BCDO2 was cloned into the vector pTrcHis (Invitrogen). The plasmid was then transformed into *Escherichia coli* BL21. Protein expression and tests for enzymatic activity were carried out as described previously (20). Tests were stopped by the addition of 100 μl water and 400 μl acetone. Lipophilic compounds were extracted with 400 μl diethyl ether and 100 μl petroleum ether. HPLC analysis was performed on a normal-phase Zorbax Sil (5 μm, 4.6×150 mm) column (Agilent, Santa Clara, CA, USA). Chromatographic separation was achieved by isocratic flow of 30% ethyl acetate/hexane at a flow rate of 1.4 ml/min. Carotenoids were extracted from tissues and plasma under a dim red safety light (600 nm). For quantification of molar amounts of carote-

noids, the HPLC was scaled with the authentic zeaxanthin and lutein (Wild, Eppelheim, Germany). Owing to a lack of 3-dehydrolutein and zeaxanthin standards, molar amounts of these compounds were calculated by using the lutein and zeaxanthin standards, respectively.

Tandem mass spectrometry (MS/MS)

Carotenoids and their metabolites were separated on an 1100 Agilent HPLC series equipped with diode-array detector and Zorbax Eclipse XDB C-18 (5 μm, 4.6×150 mm) column (Agilent), equilibrated with 50% acetonitrile in methanol. The elute at a flow rate of 1 ml/min was directed into a LXQ linear ion trap mass spectrometer (Thermo Scientific, Waltham, MA, USA) through atmospheric pressure chemical ionization (APCI) source working in the positive mode. To ensure optimal sensitivity, the instrument was tuned either for zeaxanthin or lutein. Alternatively, carotenoids and products of BCDO2 enzymatic activity were analyzed on a normal phase Zorbax Sil (5 μm, 4.6×150 mm) column (Agilent). Chromatographic separation was achieved by isocratic flow of 30% ethyl acetate/hexane at a flow rate of 1.4 ml/min. The mobile phase was directed into the mass spectrometer *via* the APCI source.

BCDO2 plasmid construction for expression in Cos7 and HepG2 cells

Total RNA (1 μg) from mouse liver was reverse transcribed by using the SuperScript One-Step RT-PCR for LongTemplates system (Invitrogen). The full-length BCDO2 open reading frame (ORF) was amplified by using the BCDO2 forward primer (5′-ATGTTGGGACCGGAAGCAGAGC-3′) and the BCDO2 reverse primer (5′-GATAGGCACAAAGGTGCC-3′) with the Expand High Fidelity PCR system (Roche, Indianapolis, IN, USA). The amplified *BCDO2* cDNA product was then cloned in frame into the pCDNA 3.1 V5/His TOPO (Invitrogen). Appropriate construction of the WT *BCDO2* (pBCDO2-WT) in the pCDNA 3.1 V5/His vector was verified by sequence analysis of both strands (Genomics Core Sequencing Facility, Case Western Reserve University, Cleveland, OH, USA).

Cell lines, cell culture, and transient transfections

Human hepatocyte HepG2 and monkey kidney COS7 cells were maintained in high-glucose DMEM supplemented with 10% FBS and 1% penicillin-streptomycin sulfate, and cultured at 37°C with 5% CO_2. For BCDO2 subcellular localization studies, COS7 cells were seeded at 50–70% confluence on glass coverslips in 6-well plates. The next day, cells were transfected with 4–6 μg of purified plasmid DNA (pBCDO2-WT) using Lipofectamine 2000 (L2000) and OptiMEM, as described previously (21). At 40–48 h post-transfection, cells were subjected to indirect immunofluorescence analysis as outlined below.

Indirect immunofluorescence and confocal microscopy

Approximately 40–48 h post-transfection, cells grown on coverslips were fixed in a freshly prepared mixture of 4% formalin in PBS (137 mM NaCl, 2.7 mM KCl, 10 mM sodium phosphate dibasic, and 2 mM potassium phosphate monobasic, pH 7.4) for 20 min at room temperature and processed as described before (21). Subcellular localization of the pBCDO2-WT in COS7 cells was achieved by exposure to the anti-V5 primary antibody (which detects the V5-tagged pBCDO2-WT) followed by the anti-rabbit conjugated Alexa 594 secondary antibody. Cells were examined under a Zeiss LSM 510 UV Meta confocal microscope with an HCX Plan ×40 numerical aperture 1.4 oil immersion objective lens (Zeiss, Jena, Germany). Images were acquired with the Zeiss confocal software, version 2.0. All experiments were carried out in triplicate. Approximately 100 cells from 10–15 fields were counted per experiment.

Analysis of reactive oxygen species (ROS) in HepG2 cells and JC-1 stain of mitochondria

Intracellular generation ROS in live cells was measured by using the Image-iT LIVE reactive oxygen species kit (Invitrogen). Human hepatocytes, namely HepG2 cells, were seeded in DMEM in 12-well dishes at 70–80% confluence and allowed to adhere overnight. Next day, the medium was replaced, and cells were treated with the vehicle only control (DMSO and THF), parent carotenoids (2 μM in 0.1% THF), or 3-dehydrocarotenoids (0.5–2 μM in 0.1% THF), the last extracted from livers of $BCDO2^{-/-}$ mice supplemented with carotenoids. Treated cells were then incubated for 2 h at 37°C and 5% CO_2, before labeling with carboxy-H_2DCFDA (Invitrogen), which emits a bright green fluorescence when oxidized by ROS. For quantification, cells were harvested by centrifugation, redissolved in 1 ml PBS. Fluorescence was determined at the emission of light at 525 nm and measured in absorbance units per milligram of protein. All experiments were carried out in duplicate and repeated 3 times. Alternatively, after exposure to carotenoids for 2 h, the changes in mitochondrial membrane potentials were assessed by using the fluorescent cationic dye, 5,5′,6,6′-tetrachloro-1,1′,3,3′-tetraethylbenzamidazolocarbocyaniniodide, commonly known as JC-1 dye (MitoPT-JC1 assay kit; Immunochemistry Technologies, Bloomington, MN, USA). Control cells were treated with 0.1% DMSO and vehicle (0.1% tetrahydrofuran). Fluorescence images were taken under a Zeiss LSM 510 UV Meta confocal microscope with an HCX Plan ×40 numerical aperture 1.4 oil-immersion objective lens. Images were acquired with Zeiss confocal software, version 2.0.

Mitochondria isolation and measurements of oxygen consumption

Mitochondria, were isolated from livers of age- and sex-matched WT or $BCDO2^{-/-}$ mice maintained either on a control or carotenoid-rich diet. Tissue homogenates were subjected to differential centrifugation in 220 mM mannitol, 70 mM sucrose, and5 mM MOPS (pH 7.4), as described previously (22). Citrate synthase was measured to ensure that each sample had comparable amounts of functional mitochondria. Oxygen consumption was measured with a Clark-type oxygen electrode in a closed chamber containing 500 μl of reaction solution (80 mM KCl, 50 mM MOPS, 5.0 mM P_i, 1.0 mM EGTA, and 1 mg of defatted BSA) at 30°C as described previously (22). Briefly, oxygen consumption was measured with glutamate (complex I), or with rotenone and succinate (complex II), rotenone and duroquinol (complex III), and rotenone, *N,N,N′,N′*-tetramethyl-*p*-phenylenediamine, and ascorbate (complex IV). To determine state 3 (ADP-dependent) respiration, 10 mM ADP was added; 100 mM ADP was used to determine maximal ADP-dependent respiration rates, and dinitrophenol (DNP) was used to determine respiration rates uncoupled from ATP synthesis.

RNA isolation and qRT-PCR analysis

RNA isolation was performed as described previously (21). qRT-PCR was carried out using the TaqMan chemistry and

Assays on Demand probes (Applied BioSystems) for mouse BCDO2 (Mm00460051_m1). The 18S rRNA (4319413E) probe set (Applied BioSystems) was used as the endogenous control. All real-time experiments were done with the ABI Step-One Plus qRT-PCR machine (Applied BioSystems).

Immunoblotting analyses

Total protein from mouse tissue was isolated, and quantitative immunoblot analysis was performed as described previously (21). Antiserums used were anti-BCDO2, anti-phospho-AKT, anti-phospho-MAPK, and anti-COX IV (all at 1:1000 dilution) or anti-MnSOD and anti-HIF1α (both at 1:2000 dilution), or anti-RAN antibody (1:5000 dilution). All figures showing quantitative analyses include data obtained from ≥2 independent experiments.

RESULTS

BCDO2 is a mitochondrial protein

Analysis of the human cardiac mitochondrial proteome indicates that BCDO2 is a mitochondrial protein (23). To verify a mitochondrial localization, we expressed the murine BCDO2 as a tagged protein in COS7 cells. Immunostaining and confocal imaging revealed that BCDO2 was distributed in cells in a pattern that resembled staining for mitochondria (**Fig. 1*A***). We performed coimmunostaining for cytochrome-*c* oxidase IV (COXIV), a well-known mitochondrial protein marker. Merged images showed that BCDO2 colocalized with COXIV, confirming the mitochondrial localization for this enzyme (Fig. 1*A*).

BCDO2 catalyzes oxidative cleavage at the 9,10 and 9′,10 positions of various carotenoids

To define substrate specificity of BCDO2, we expressed the murine enzyme as a recombinant protein in *E. coli* and performed assays with carotenes and xanthophylls. β-10′-Apocarotenal was formed from β,β-carotene in these assays (Supplemental Fig. S1). In addition, a compound with spectral characteristics of rosafluene

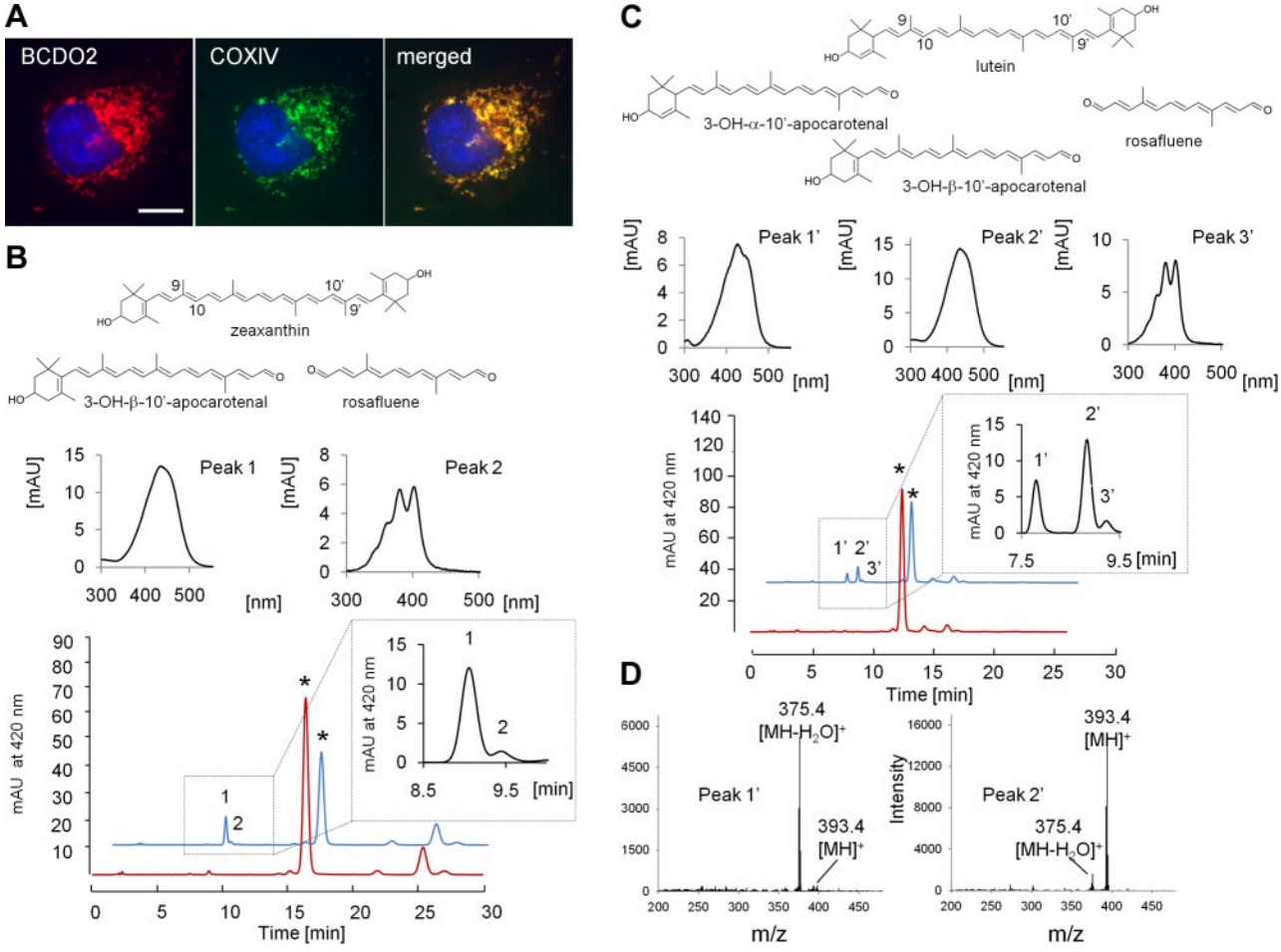

Figure 1. BCDO2 is a mitochondrial protein that metabolizes xanthophylls. *A*) COS7 cells expressing murine BCDO2 with a V5 tag. Immunostaining was performed using anti-V5 antibody for BCDO2 (left panel) and anti-COXIV antibody (middle panel). Merged image (right panel) shows mitochondrial colocalization of BCDO2 with COXIV. Scale bar = 10 μm. *B*, *C*) HPLC profiles at 420 nm of a lipid extract from *in vitro* tests for BCDO2 enzymatic activity. Reaction was carried out with 20 μM zeaxanthin (*B*) and lutein (*C*) at 28°C for 10 s (red trace) and 10 min (blue trace). Insets: enlargement of sectors of peaks 1 (3-OH-β-10′-apocarotenal) and 2 (rosafluene) (*B*) and peaks 1′ (3-OH-ε-10′-apocarotenal), 2′ (3-OH-β-10′-apocarotenal), and 3′ (rosafluene) (*C*). Spectral characteristics of peaks are presented above HPLC traces. *D*) Mass spectra from peaks 1and 2′. Note that 3-OH-ε-10′-apocarotenal loses water on ionization. Therefore, *m/z* = 375.4 MZ is the dominant ion.

was present. This C14-dialdehyde results from the removal of both β-ionone ring sites of β,β-carotene at positions 9,10 and 9′,10′ (24). We next tested β-cryptoxanthin, an asymmetric carotenoid with one β-ionone and one 3-OH-β-ionone ring. Interestingly, β-10′-apocarotenal was produced from this substrate (Supplemental Fig. S2), indicating that BCDO2 also catalyzes the removal of 3-OH-β-ionone rings. Zeaxanthin, with two 3-OH-β-ionone rings, was also efficiently converted, and two different cleavage products became detectable (Fig. 1*B*). Spectral characteristics and a molecular mass of 392.4 Da (m/z=393.4 $[MH]^+$) indicated that one of these products was 3-OH-β-10′-apocarotenal, formed by the removal of one 3-OH-β-ionone site at position 9,10. Again, rosafluene was produced that resulted from the removal of both ionone ring sites at position 9,10 and 9′,10′, and we also detected 3-OH-β-ionon (Supplemental Fig. S3). Tests with lutein with a 3-OH-β- and 3-OH-ε-ionone ring as a substrate revealed another enzymatic property of BCDO2. Both the β- and ε-3-OH-10′-apocarotenal cleavage products became detectable by their spectral characteristics and molecular masses of 392.4 Da (m/z=393.4 $[MH]^+$ and 375.4 $[MH\text{-}H_2O]^+$) (Fig. 1*C*, *D*). In addition, rosafluene was produced (Fig. 1*C*). Thus, BCDO2 displayed broad substrate specificity and catalyzed oxidative cleavage both at position 9,10 and 9′,10′ position of the carbon backbone of carotenes and xanthophylls.

Carotenoid metabolism is impaired in BCDO2-KO mice

To analyze the physiological function of BCDO2, we established a *BCDO2*-KO mouse model by replacing exons 1 to 4 and part of exon 5 of the *BCDO2* gene with an NLS-lacZ/neo cassette (Supplemental Fig. S4*A*). Wild-type and mutated alleles were routinely identified by genomic PCR using specific primer pairs (Supplemental Fig. S4*B*), and we confirmed the ablation of BCDO2 at the protein level in isolated hepatic mitochondria (Supplemental Fig. S4*C*). $BCDO2^{-/-}$ mice developed normally, and both females and males were fertile when raised on standard mouse chow. We treated 5-wk-old $BCDO2^{-/-}$ and WT mice for 8 wk with diets supplemented with 50 mg/kg zeaxanthin or lutein. In addition, we treated HET mice with a diet supplemented with 50 mg/kg zeaxanthin. We chose these xanthophylls because they cannot be metabolized by BCMO1 that is still expressed in BCDO2-deficient mice. On dietary supplementation, a consequence of BCDO2 deficiency was readily apparent on gross abdominal sectioning. $BCDO2^{-/-}$ but not WT mice showed a yellow coloring of adipose tissues (**Fig. 2*A***). HPLC analysis of lipid extracts of livers revealed that only small amounts of zeaxanthin or lutein were present in $BCDO2^{-/-}$ mice, but these mice accumulated large amounts of metabolites of these carotenoids, with characteristically changed retention times and absorption spectra (Fig. 2*B–D* and Supplemental Fig. S5). Formation of these compounds was also obvious in HET animals and to a lesser extent in WT mice (Fig. 2*D* and Supplemental Fig. S5). In $BCDO2^{-/-}$ animals fed supplemental zeanthin, one major zeaxanthin derivative was found (Fig. 2*B*), whereas in animals fed supplemental lutein, three different lutein derivatives with similar spectral characteristics were present (Fig. 2*C*). We performed LC-MS/MS to identify the chemical identity of these compounds. The zeaxanthin derivative had a molecular mass of 564.5 Da (m/z=565.5 MH^+) and thus had lost 4 mass units as compared to parent zeaxanthin. The MS/MS fragmentation pattern clearly indicated that this compound was 3,3′-didehydrozeaxanthin, in which both 3-hydroxy groups were oxidized to the corresponding oxo derivatives (**Fig. 3*A***). In the lutein-supplementation group, a compound with the same molecular mass but a different fragmentation pattern indicative of 3,3′-didehydrolutein formation was observed (Fig. 3*B*). Another lutein derivative characterized by mass of 548.5 (m/z=489.5 $[MH]^+$) displayed a fragmentation pattern that permitted its identification as 3-dehydro-α-carotene (Fig. 3*B*). On this HPLC system, we could not detect the third lutein derivative (Fig. 2*C*), indicating that the reversed-phase column was limited in the resolution of lutein derivatives. These carotenoid metabolites were detectable in different concentrations in all tissues examined, including the blood, heart, and liver (Fig. 2*D* and Supplemental Fig. S5). Notably, we found no accumulation of apocarotenoid cleavage products in WT mice, indicating that these compounds are rapidly further metabolized and/or secreted.

Carotenoids impair mitochondrial function in BCDO2-deficient mice

To analyze consequences of carotenoid accumulation, we focused on liver pathophysiology. In the livers of WT mice, *BCDO2* mRNA expression increased 7-fold on zeaxanthin supplementation, as compared to age-matched animals raised on a chow diet (**Fig. 4*A***). Interestingly, induction of *BCDO2* mRNA expression was not seen in HET animals, which also accumulated dehydrocarotenoids. Histological analysis of livers revealed that HET $BCDO2^{+/-}$ and homozygous $BCDO2^{-/-}$ but not WT mice developed liver steatosis with large lipid droplets in hepatocytes and a significantly increased triacylglyceride content (Fig. 4*B*, *C*). This phenotype was not evident in age-matched $BCDO2^{-/-}$ mice raised on a chow diet, indicating that this liver pathology was induced by carotenoid supplementation (Fig. 4*B*).

Hepatic mitochondria isolated from $BCDO2^{-/-}$ mice fed the lutein diet showed a strong yellow coloring, and HPLC analysis revealed the accumulation of 3-dehydrocarotenoids (Fig. 4*D*). Carotenoids are rigid lipophilic molecules with an extended polyene chromophore that can act as an electron sink (1). Therefore, we speculated that carotenoid accumulation may interfere with mitochondrial function. To provide evidence for this hypothesis, we screened for expression of manganese superoxide dismutase (MnSOD), which is a reliable indicator of mitochondrial stress and dysfunction (25). Immunoblot analysis showed a 9-fold induction of MnSOD in hepatic mitochondria of carotenoid-supplemented BCDO2-defi-

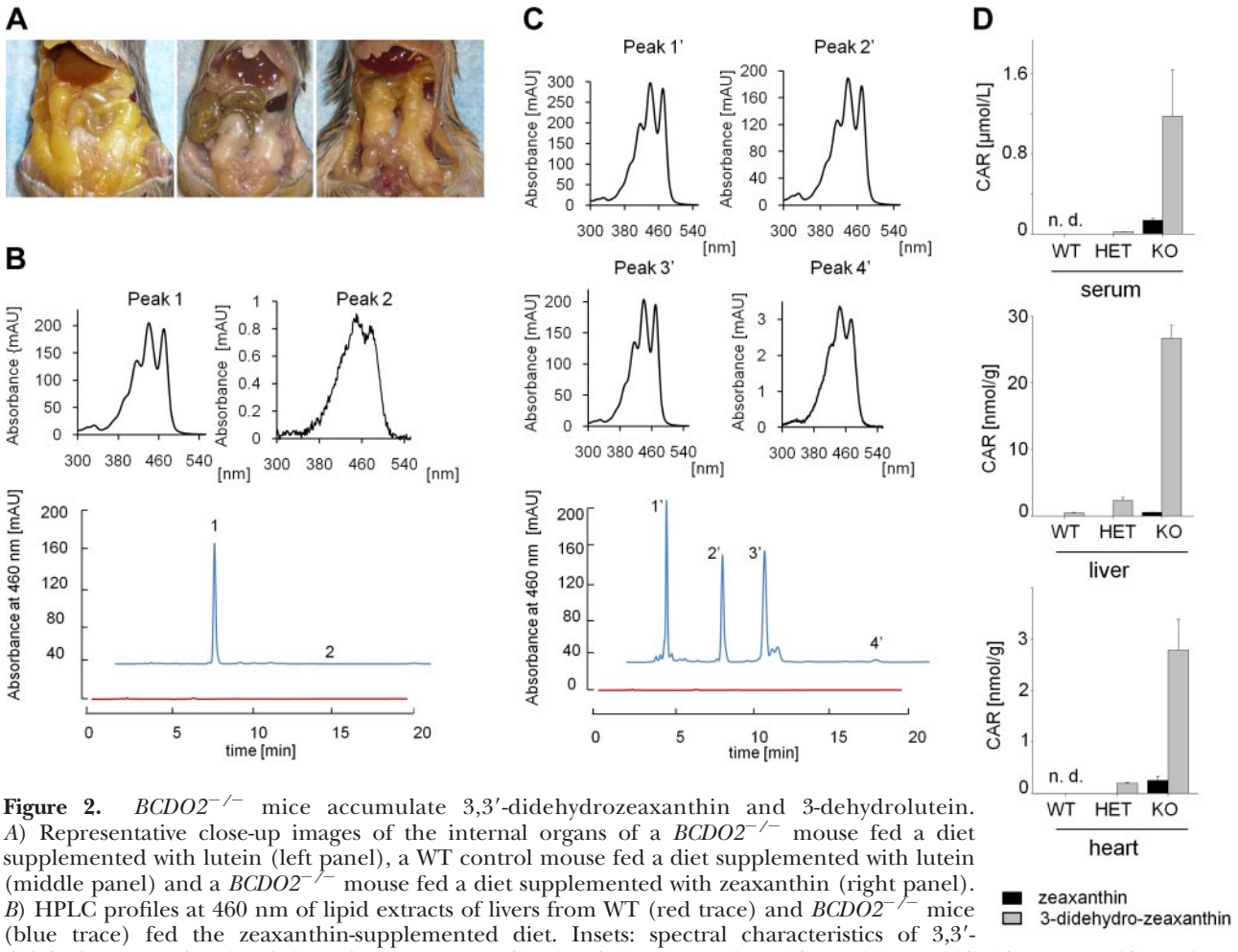

Figure 2. *BCDO2*$^{-/-}$ mice accumulate 3,3′-didehydrozeaxanthin and 3-dehydrolutein. *A*) Representative close-up images of the internal organs of a *BCDO2*$^{-/-}$ mouse fed a diet supplemented with lutein (left panel), a WT control mouse fed a diet supplemented with lutein (middle panel) and a *BCDO2*$^{-/-}$ mouse fed a diet supplemented with zeaxanthin (right panel). *B*) HPLC profiles at 460 nm of lipid extracts of livers from WT (red trace) and *BCDO2*$^{-/-}$ mice (blue trace) fed the zeaxanthin-supplemented diet. Insets: spectral characteristics of 3,3′-didehydrozeaxanthin (peak 1) and parent zeaxanthin (peak 2). *C*) HPLC profiles at 460 nm of lipid extracts of livers from WT (red trace) and *BCDO2*$^{-/-}$ mice (blue trace) fed a diet supplemented with lutein. Insets: spectral characteristics of 3-dehydrolutein metabolites (peaks 1′–3′) and parent lutein (peak 4′). Two of these compounds were identified by MS analysis (see Fig. 3*B*). *D*) Molar amounts of zeaxanthin and 3,3′-didehydrozeaxanthin in the serum, liver, and heart of WT, *BCDO2*-HET, and *BCDO2*-KO mice. Carotenoid content (CAR) was determined by HPLC analysis. Values represent means ± SD of 5 animals.

cient animals (Fig. 4*E*). We then compared respiration rates in hepatic mitochondria isolated from 13-wk-old male *BCDO2*$^{-/-}$ mice fed either with lutein diet or the same diet without lutein supplementation (control diet) for 8 wk. Citrate synthase was initially measured to ensure that each preparation had comparable amounts of functional mitochondria (**Table 1**). Oxygen consumption then was measured with substrates for complex I, II, III, and IV (Table 1 and Fig. 4*F*). State 3 (ADP-dependent) respiration, as well as respiration with high ADP, was decreased in *BCDO2*$^{-/-}$ mice fed the lutein diet compared to *BCDO2*$^{-/-}$ mice fed the control diet (Fig. 4*F* and Table 1). Uncoupling of respiration by dinitrophenol did not ameliorate this defect, indicating that carotenoid accumulation directly interfered with the electron transport chain (Table 1). In addition, ADP/oxygen rate, a measure for the efficiency of oxidative phosphorylation, was not reduced (Table 1). In both sets of mitochondria, state 4 (ADP-independent) respiration and respiratory control ratios were unchanged (Fig. 4*F* and Table 1), showing that mitochondria were structurally intact.

Carotenoids induce ROS production and depolarize mitochondrial membranes

Disturbances in the mitochondrial electron transport chain generally result in the production of ROS (25). To test whether carotenoids can induce ROS production, human liver HepG2 cells were treated with the zeaxanthin and lutein or their 3-dehydro derivatives isolated from livers of supplemental zeaxanthin- and lutein-treated *BCDO2*$^{-/-}$ mice (**Fig. 5**). After 2 h incubation, carboxy-H_2DCFDA dye was added for detection of ROS, and cells then were examined by microscopy. Treatment of HepG2 cells with carotenoids resulted in green fluorescence, indicative of ROS production (Fig. 5*A–F*). ROS production was most pronounced on treatment with 3-dehydrocarotenoids and was dose dependently increased (0.1–2.0 µM). Cells treated with 2 µM zeaxanthin and lutein showed modest fluorescence (Fig. 5*B, E*), but vehicle-treated cells showed none (Fig. 5*A*). By quantification of fluorescence, we showed that the induction of oxidative stress was dose dependent

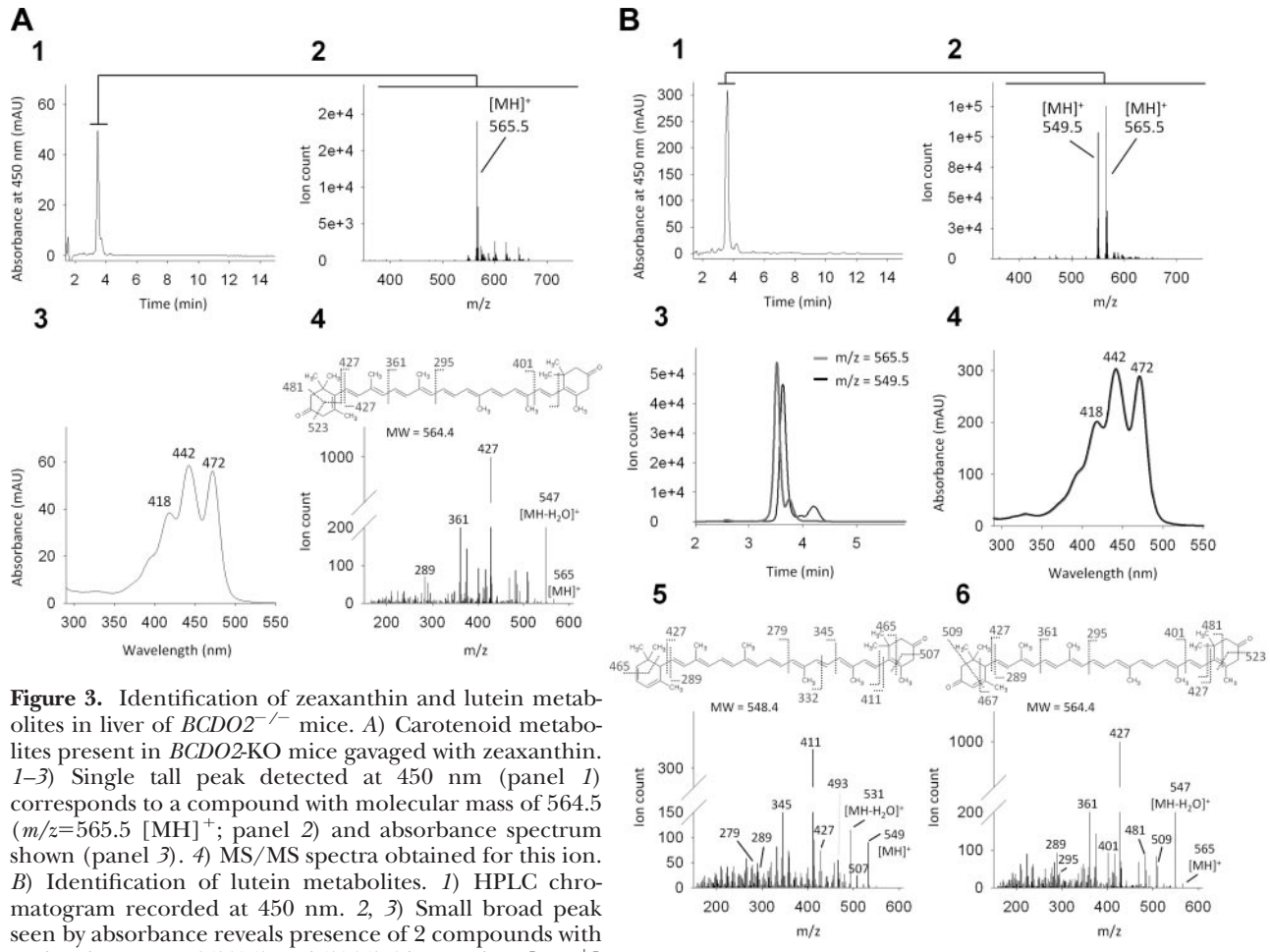

Figure 3. Identification of zeaxanthin and lutein metabolites in liver of *BCDO2*$^{-/-}$ mice. *A*) Carotenoid metabolites present in *BCDO2*-KO mice gavaged with zeaxanthin. *1–3*) Single tall peak detected at 450 nm (panel *1*) corresponds to a compound with molecular mass of 564.5 (*m/z*=565.5 $[MH]^+$; panel *2*) and absorbance spectrum shown (panel *3*). *4*) MS/MS spectra obtained for this ion. *B*) Identification of lutein metabolites. *1*) HPLC chromatogram recorded at 450 nm. *2, 3*) Small broad peak seen by absorbance reveals presence of 2 compounds with molecular mass of 548.5 and 564.5 (detected as $[MH^+]$ ions) as observed in MS spectrum (panel *2*) and extracted ion chromatogram (panel *3*). *4*) Both compounds share a similar absorbance spectrum characterized by their distinctive absorbance maxima. *5, 6*) Chemical structures of the detected compounds with molecular masses of 548.5 (panel *5*) and 564.5 (panel *6*) were deducted from MS/MS fragmentation spectra.

and already occurred at concentrations of 0.1 μM with didehydrozeaxanthin (Fig. 5*G*). We next wondered whether other carotenoids, such as β,β-carotene, can also induce ROS production in this cell line. Treatment of cells with β,β-carotene also resulted in strong green fluorescence compared to vehicle (Fig. 5*H, J*). Transfection of HepG2 cells with an expression vector for recombinant murine BCDO2 significantly reduced ROS production on β,β-carotene treatment (Fig. 5*K, L*).

To measure whether carotenoids can influence mitochondrial membrane potential, we took advantage of the JC-1 stain. The JC-1 dye enters intact mitochondria, where it aggregates and fluoresces red (**Fig. 6*A***). When the membrane potential collapses, JC-1 no longer accumulates in mitochondria and is dispersed throughout the cytoplasm and fluoresces green (Fig. 6*B*). Cells treated with 3-dehyrocarotenoids showed strong green fluorescence for monomeric JC-1, indicative for loss of mitochondrial membrane potential (Fig. 6*C*). Green fluorescence was also observed in cells treated with zeaxanthin or β,β-carotene (Fig. 6*D, E*). Expression of recombinant BCDO2 ameliorated membrane depolarization in β,β-carotene-treated cells (Fig. 6*F*). Thus, all tested carotenoids impaired mitochondrial function and induced ROS production.

Major stress pathways are induced by carotenoids in *BCDO2*$^{-/-}$ mice

ROS can activate key signaling pathways for cell proliferation and inflammation that are related to cancer and cardiovascular disease. Therefore, we assessed protein levels of key components of oxidative stress-regulated pathways, including HIF1α, MAPK, and AKT (26). Analysis of HIF1α protein levels in livers of animals maintained on a zeaxanthin diet showed a 5- and 7-fold increase in *BCDO2*$^{+/-}$ and *BCDO2*$^{-/-}$ mice, respectively, compared to WT mice (Fig. 6*G*). For the phosphorylation of MAPK, we utilized an antibody that recognizes the activating phosphorylation of residues Thr187 and Thr189 of the p44-MAPK and the equivalent phosphorylation of p42-MAPK. For AKT phosphorylation, we employed an antibody that recognizes the phosphorylation of Ser473. Analysis of total protein isolated from the livers of *BCDO2*$^{+/-}$ and *BCDO2*$^{-/-}$ mice maintained on a zeaxanthin diet showed an 8- and

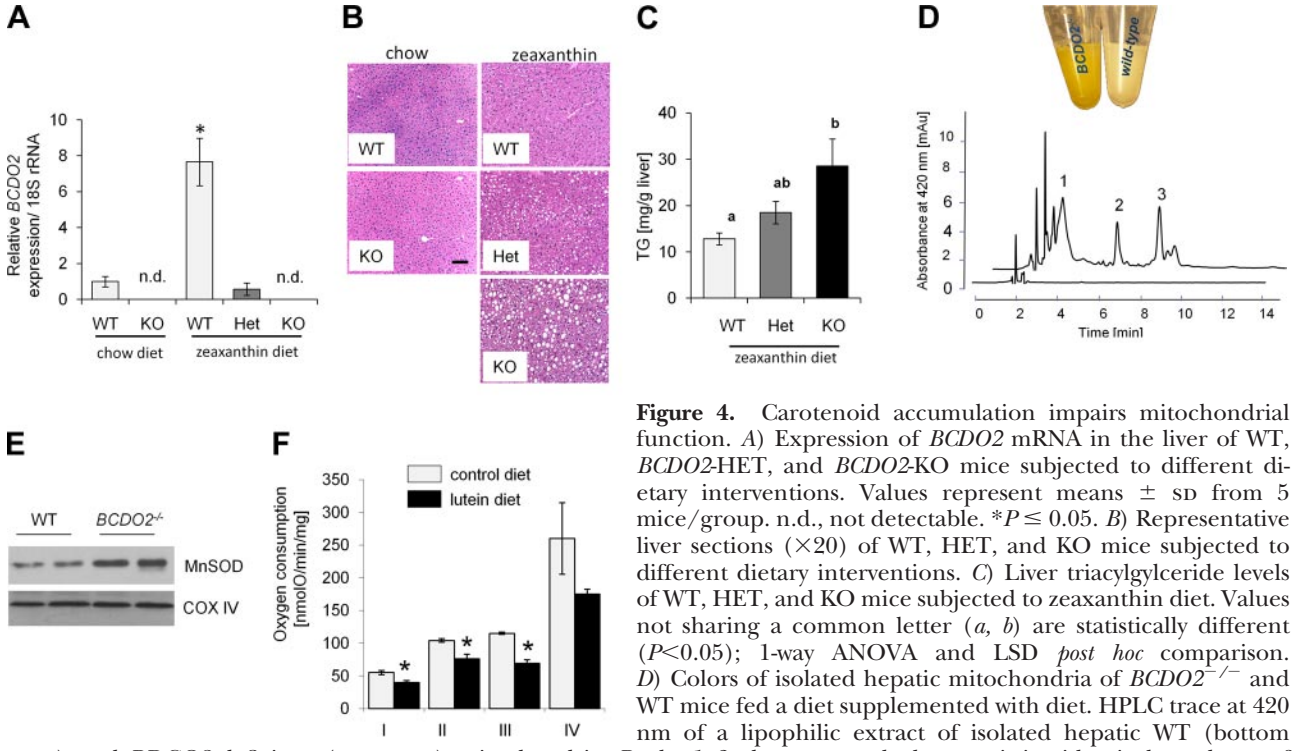

Figure 4. Carotenoid accumulation impairs mitochondrial function. *A*) Expression of *BCDO2* mRNA in the liver of WT, *BCDO2*-HET, and *BCDO2*-KO mice subjected to different dietary interventions. Values represent means ± SD from 5 mice/group. n.d., not detectable. $*P \leq 0.05$. *B*) Representative liver sections (×20) of WT, HET, and KO mice subjected to different dietary interventions. *C*) Liver triacylgylceride levels of WT, HET, and KO mice subjected to zeaxanthin diet. Values not sharing a common letter (*a, b*) are statistically different ($P<0.05$); 1-way ANOVA and LSD *post hoc* comparison. *D*) Colors of isolated hepatic mitochondria of *BCDO2*$^{-/-}$ and WT mice fed a diet supplemented with diet. HPLC trace at 420 nm of a lipophilic extract of isolated hepatic WT (bottom trace) and BDCO2-deficient (top trace) mitochondria. Peaks 1–3 show spectral characteristics identical to those of 3-dehyrolutein derivatives depicted in Fig. 2*C*. *E*) Immunoblot analysis for MnSOD with protein extracts from hepatic mitochondria (50 μg protein/lane). Staining for COXIV was used as a loading control. *F*) Oxygen consumption of complexes I–IV in isolated hepatic mitochondria from age-matched male *BCDO2*$^{-/-}$ mice fed lutein diet *vs.* control diet. Oxygen consumption was measured by the addition of complexes I–IV (see Materials and Methods) in the presence of 100 mM ADP to determine maximal ADP-dependent respiration rates. $*P \leq 0.05$.

9-fold induction of phospho-AKT and 8- and 9-fold induction of phospho-MAPK, as compared to WT mice fed the same diet (Fig. 6*G*). On the standard chow diet, *BCDO2*$^{-/-}$ mice showed a small induction of phospho p42-MAPK, but no increase in phosphorylation at Ser473 of AKT (Fig. 6*G*). Since 3-dehydrocarotenoid-accumulation was evident in other tissues, we also measured phospho-AKT and phospho-MAPK levels in the heart. In this tissue, a marked induction of 8- and 9-fold of phospho-AKT and 6- and 7-fold of phospho-MAPK enzymes was evident in supplemental zeaxanthin-treated *BCDO2*$^{-/-}$ and *BCDO2*$^{+/-}$ mice, respectively (Fig. 6*H*). No alterations of these levels became detectable in the hearts of animals fed nonsupplemented diets, indicating that these markers of oxidative stress were induced in additional tissues by carotenoid accumulation.

DISCUSSION

Here, we identified the carotenoid-oxygenase BCDO2 as a mitochondrial enzyme that converts both β,β-

TABLE 1. *Respiration rates of complex I of hepatic mitochondria isolated from BCDO2*$^{-/-}$ *mice subjected to control or lutein diet feeding for 8 wk*

Parameter	Control diet	Lutein diet
State 3 (nmol O/min/mg protein)	57 ± 1.6	42 ± 3.2*
State 4 (nmol O/min/mg protein)	5.7 ± 1.8	5.2 ± 1.8
Respiratory control ratio	12.1 ± 3.3	11.2 ± 4.7
ADP/O ratio	2.2 ± 0.08	2.6 ± 0.10*
High ADP (nmol O/min/mg protein)	55 ± 3.1	40 ± 2.8*
Uncoupled rate (nmol O/min/mg protein)	55 ± 2.6	38 ± 2.1*
Citrate synthase (nmol/min/mg mitochondrial protein)	156 ± 5.3	188 ± 18

Oxygen consumption in isolated hepatic mitochondria was measured with glutamate (complex I), or with rotenone and succinate (complex II), rotenone and duroquinol (complex III), and rotenone, *N,N,N′,N′*-tetramethyl-*p*-phenylenediamine, and ascorbate (complex IV). To determine state 3 (ADP-dependent) respiration, 10 mM ADP was added; 100 mM ADP was used to determine maximal ADP-dependent respiration rates (high ADP), and dinitrophenol (DNP) was used to determine respiration rates uncoupled from ATP synthesis. Values represent means ± SD of hepatic mitochondria preparations from 3 animals/genotype. $*P < 0.05$; *t* test.

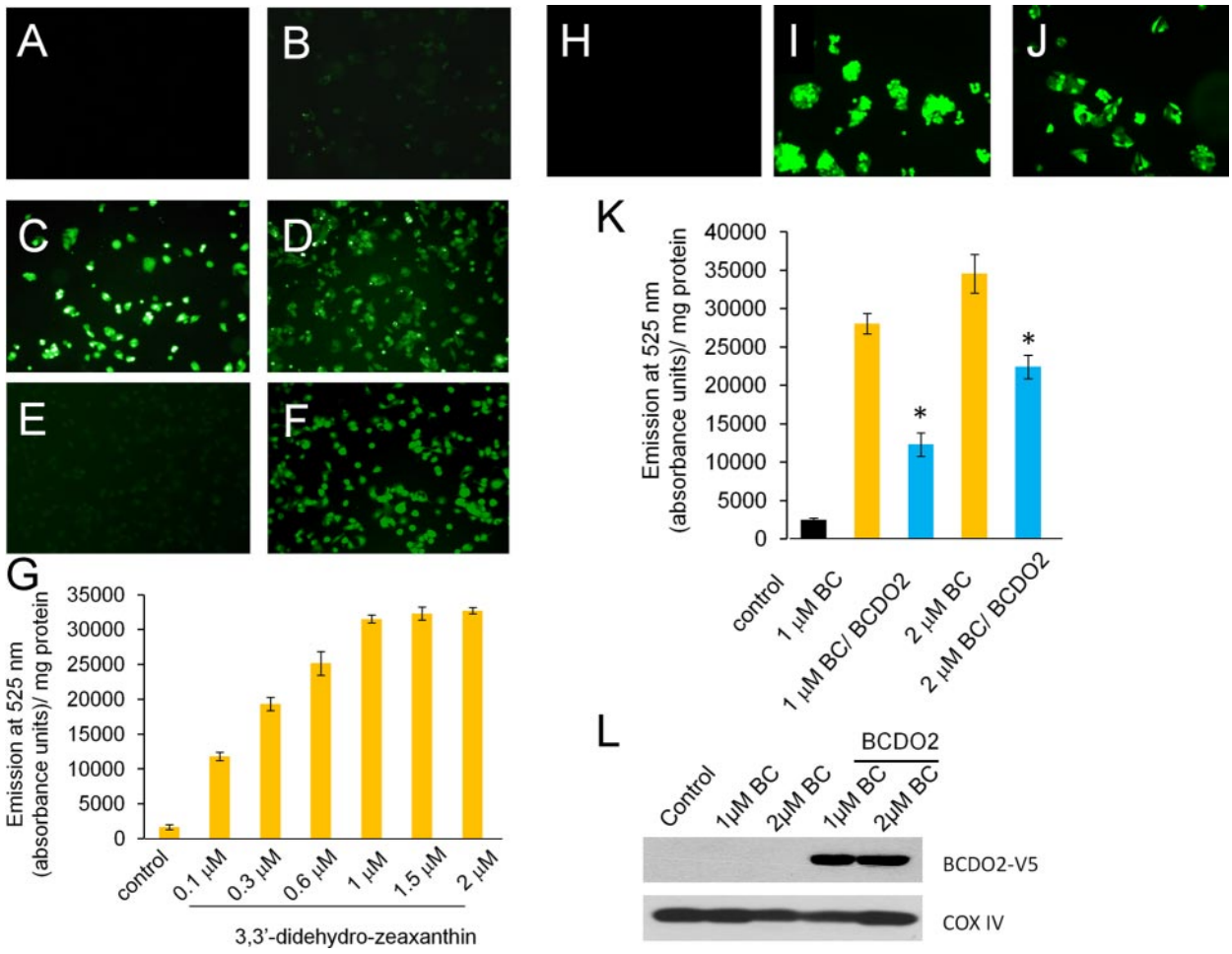

Figure 5. Carotenoids induce ROS production in HepG2 cells. *A–F*) HepG2 cells were treated with vehicle only (*A*), 2 μM zeaxanthin (*B*), 0.5 μM 3,3′-didehydrozeaxanthin (*C*), 2 μM 3,3′-didehydrozeaxanthin (*D*), 2 μM lutein (*E*), or 2 μM dihydrolutein derivatives (*F*). After 2 h of incubation, the nonfluorescent carboxy-H_2DCFDA dye was added to treated cells. In the presence of ROS, the reduced fluorescein compound is oxidized and emits bright green fluorescence. Representative images were taken under a fluorescent microscope at ×20. *G*) HepG2 cells were treated with increasing amounts of 3,3′-didehydrocarotenoids (0.1, 0.3, 0.6, 1.0, 1.5, and 2 μM), respectively. Treated cells were harvested by centrifugation and resuspended in 1× PBS. Fluorescence was determined by emission of light at 525 nm and measured in absorbance units per milligram of protein. Assay was performed in duplicate and repeated 3 times. *H, I*) HepG2 cells were treated with vehicle only (*H*) or 2 μM of β,β-carotene (*I*). *J*) HepG2 cells were transfected with a vector for the expression of murine BCDO2. After 2 d, cells were treated with 2 μM of β,β-carotene. After 2 h, nonfluorescent carboxy-H_2DCFDA dye was added to treated cells (*H–J*). Representative images were taken under a fluorescent microscope at ×40. *K*) Nontransfected HepG2 cells and HepG2 cells transfected with a plasmid for recombinant murine *BCDO2* expression were treated with different amounts of β,β-carotene. After 2 h, nonfluorescent carboxy-H_2DCFDA dye was added, and cells were harvested by centrifugation and redissolved in 1× PBS. Fluorescence was determined by emission of light at 525 nm. Data represent values from 3 experiments. $^*P < 0.05$. *L*) Immunoblot analysis of HepG cells from *K* confirms the expression of recombinant murine V5-tagged BCDO2. In addition, levels of the mitochondrial marker protein COXIV indicate that amounts of mitochondria are not grossly altered on overexpression of recombinant BCDO2.

carotene and xanthophylls to apocarotenoid breakdown products. Studies in BCDO2-deficient mice showed that BCDO2 plays an important role for protecting against carotenoid-induced mitochondrial dysfunction. In this mouse model, accumulated carotenoids impaired mitochondrial respiration and induced cellular signaling pathways related to oxidative stress and disease. Administration of carotenoids to human HepG2 cells depolarized mitochondrial membranes and resulted in the production of ROS. Thus, in contrast to their protective role in photosynthetic membranes, carotenoids can interfere with mitochondrial function. Mammalian cells thus express a mitochondrial carotenoid-oxygenase to protect these vital organelles.

BCDO2 is a mitochondrial enzyme that displays broad substrate specificity

Mammalian genomes encode 3 related proteins that belong to an ancestral family of carotenoid-cleaving enzymes (5). The structures of RPE65 and a bacterial apocarotenoid-oxygenase recently have been solved

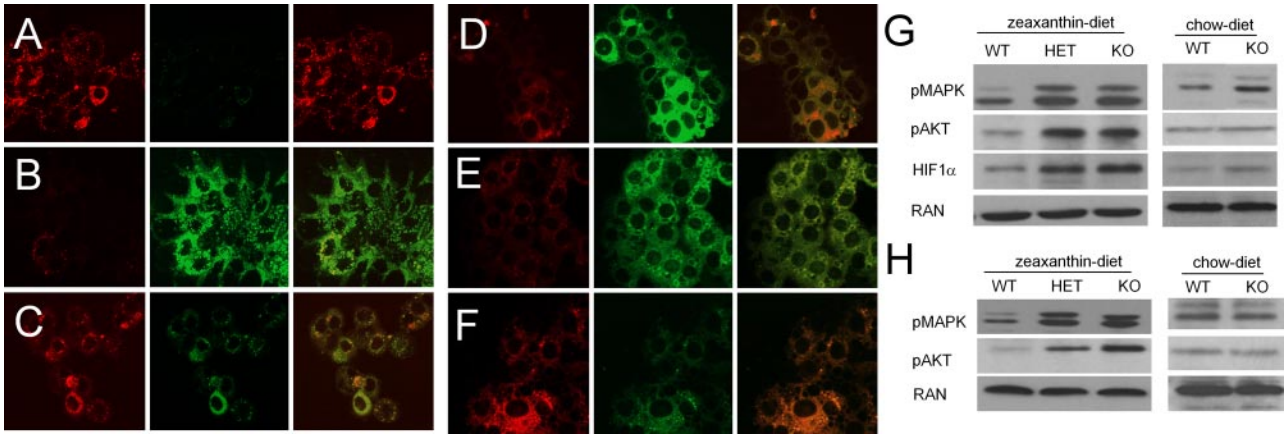

Figure 6. Carotenoids can depolarize mitochondrial membrane potential in HepG2 cells and induce signaling pathways related to oxidative stress in mice. *A–F*) HepG2 cells were treated with vehicle (*A*), 5 μM carbonylcyanide *m*-chlorophenylhydrazone as positive control (*B*), 2 μM zeaxanthin (*C*), 2 μM 3,3′-didehydrozeaxanthin (*D*), and 1 μM β,β-carotene (*E*) or were transfected with a plasmid for the expression of recombinant murine BCDO2 prior to treatment with 1 μM β,β-carotene (*F*). After 2 h of incubation, mitochondrial membrane potential was assessed by JC-1 stain. Cells were visualized under a confocal fluorescent microscope. Red fluorescence of JC-1 aggregates shows distribution of intact mitochondria (left panels). Green fluorescence of JC-1 monomers indicates mitochondria with depolarized membrane potential (middle panels). Merged images show overlays of the left and middle panel (right panels). Data were obtained from ≥3 independent experiments. Images were taken at ×20. *G, H*) Analysis of key protein markers of stress-regulated pathways, known to be induced by ROS, in liver (*G*) and heart (*H*) of age- and sex-matched animals subjected to either zeaxanthin diet or chow diet. Expression levels of phospho-MAPK 44/42 (pMAPK), phospho-AKT Ser473 (pAKT), and HIF1α were analyzed by immunoblot analysis in age-matched WT, *BCDO2*-HET, or *BCDO2*-KO animals. Fifty micrograms of protein was loaded per lane. Each lane represents pooled samples from 5 animals. Ras-related nuclear protein (RAN) was used as loading control.

(27, 28). One of the most prominent structural features of these proteins is that the active center, defined by a coordinated ferrous iron, is accessible through a large kinked tunnel. Biochemical analysis of the insect carotenoid-oxygenase NinaB revealed that the enzyme interacts with one of the two ionone ring sites of its carotenoid substrates in a positioned manner (20). For mammalian BCMO1, this interaction clearly requires a nonsubstituted β-ionone ring site, explaining its specificity for a limited number of proretinoid carotenoids, such as β,β-carotene (8). We found that BCDO2 catalyzed the conversion of both β,β-carotene and xanthophylls, such as lutein. This finding indicates that the enzyme can interact both with β- and ε-3-OH-ionone ring sites of carotenoids. In this reaction, BCDO2 removed both ionone ring sites from its substrates by oxidative cleavage at position C9,C10, and C9′,C10′, resulting in the formation of the C14-dialdehyde rosafluene and 2 inone molecules. BCDO2 has been previously shown to metabolize even noncyclic carotenoids, such as lycopene (12). We also found a marked difference in the subcellular localization of the two mammalian carotenoid-oxygenases. BCMO1 is a cytoplasm protein (8), whereas BCDO2 localized to mitochondria both *in vitro* in the experimental cell line and *in vivo*. Thus, BCDO2 is a mitochondrial protein that displays broad substrate specificity for carotenoids.

Carotenoids can impair mitochondrial function and induce oxidative stress

Animals acquire carotenoids from external sources, transport them within the body, and stabilize them in protein-bound form and in lipid droplets in target cells, such as in the eyes (29). BCDO2 is expressed in various tissues, including liver, heart, and skeletal muscle (30). To answer the question of the requirement of a mitochondrial carotenoid-oxygenase in such tissues, we established a BCDO2-deficient mouse model. In BCDO2-deficient mice, zeaxanthin and lutein accumulated in several tissues in the form of their oxidized 3-dehydro metabolites. This accumulation also was evident in HET animals, indicating that the loss of one allele causes haploinsufficiency, thus highlighting the importance of BCDO2 for carotenoid homeostasis. A production of 3-dehydrocarotenoids from xanthophylls has also been described in humans (31, 32). In WT mice, a 7-fold induction of *BCDO2* mRNA expression largely prevented this accumulation. Interestingly, we found no accumulation of apocarotenoid cleavage products, such as 3-OH-10′-apocartenoids and rosafluene, in WT mice, indicating that these compounds are rapidly degraded and/or secreted by pathways that await molecular description. Moreover, the enzymatic activity that converts xanthophylls to their 3-dehydro derivatives needs molecular and biochemical characterization.

In agreement with its subcellular localization, carotenoid accumulation was evident in isolated hepatic mitochondria in *BCDO2*$^{-/-}$ mice. In contrast, no carotenoids were detected in hepatic mitochondria of WT mice that express BCDO2. Carotenoids are lipophilic molecules with an extended polyene chromophore that can act as an electron sink (1). In addition, these rigid lipids may disturb membrane topology of mitochondria. We showed for isolated hepatic mitochondria that accumulated carotenoids directly interfered with the mitochondrial elec-

tron transport chain. ADP-dependent respiration, respiration with high ADP, and uncoupled respiration of BCDO2-deficient mitochondria were all significantly reduced in different complexes in mice fed the lutein diet. The levels of MnSOD, a classical marker for mitochondrial dysfunction, were increased 9-fold in *BCDO2*$^{-/-}$ mice as compared to WT mice fed supplemental carotenoids. Disturbances of mitochondrial electron transport chain can result in the production of ROS (25). In this context, we found that carotenoids induced ROS production in human HepG2 cells. With JC-1 staining of cells, we showed that carotenoids can even depolarize mitochondrial membrane potential in HepG2 cells. This impairment was not only induced on 3-dehydrocarotenoid treatment but also on treatments with β,β-carotene, zeaxanthin, and lutein. Expression of recombinant murine BCDO2 in HepG2 cells prior to β,β-carotene treatment significantly reduced ROS production and also protected against mitochondrial membrane depolarization. Previously, it has been reported that lycopene treatment of human cell lines can impair mitochondrial function (33). These findings explain the broad substrate specificity of BCDO2 that protects mitochondria against diverse carotenoids.

Carotenoid-induced oxidative stress also was evidenced in *BCDO2*$^{-/-}$ mice, as observed by significantly increased protein levels of HIF1α. HIF1α protein is stabilized in response to increased generation of ROS in mitochondria to activate cellular responses that counteract this condition (34). Moreover, protein levels of phosphorylated AKT and MAPK were significantly increased in the liver. These proteins are key players in oxidative stress-induced pathways that regulate various cellular activities, such as cell proliferation and cell survival/apoptosis (35, 36). Interestingly, this response also was obvious in heterozygous mice that accumulated much lower levels of carotenoids and was not just restricted to the liver but was found in the heart. The induction of pathways related to oxidative stress in the heart of heterozygous animals indicated that carotenoids can induce oxidative stress already at relatively low concentrations (0.2 nmol/g). Moreover, both heterozygous and homozygous animals accumulated triacylglycerides and developed liver steatosis, an impairment that has been associated with mitochondrial dysfunction and oxidative stress (37). Thus, BCDO2 plays a critical role for the protection of tissues against carotenoid-induced mitochondrial dysfunction that can result in oxidative stress and disease.

Implications for carotenoids in health and disease

Carotenoids are a major source for vitamin A in the human diet and act as scavengers of free radicals and filters of phototoxic blue light in certain tissues. Recent research showed mammals have evolved efficient mechanisms to control carotenoid homeostasis. A negative feedback control mechanism depending on the carotenoid-oxygenase BCMO1 has been elucidated that is responsible for adaptation of intestinal carotenoid absorption to the fluctuating levels in staple food (21). Here, we showed that the second carotenoid-oxygenase plays an even more diversified role for carotenoid homeostasis and degrades both carotenes and xanthophylls to apocarotenoid breakdown products to prevent carotenoid accumulation in mitochondria. However, large clinical trials suggest that high-dose supplementation could be harmful for smokers (for review, see ref. 38), indicating that these control mechanisms can be bypassed under certain circumstances. Studies in rats show that high doses of β,β-carotene induce ROS production in liver and other tissues (39). In ferrets, high-dose supplementation with β,β-carotene induces pathways related to cell proliferation and cancer (40). In part, this limitation is explained by relatively low turnover rates of carotenoid-oxygenases, estimated to be one carotenoid molecule per minute (20). In humans, genetic predisposition may also play a role in this process. Frequent polymorphism in the human *BCMO1* gene occurs, and afflicted individuals have increased carotenoid blood levels (15, 41, 42). For BCDO2, a single base pair polymorphism in intron 2 has been identified and correlates with altered blood levels of interleukin 18, a proinflammatory cytokine associated with type 2 diabetes and cardiovascular disease (18). Oxidative stress has been identified as a key element underlying a plethora of human disease such as cancer, diabetes, and cardiovascular and neurodegenerative disease. Thus, our findings likely explain harmful effects of high-dose carotenoid supplementation in people at risk of such disease and identify BCDO2 as a key defender against oxidative stress. Carotenoid-oxygenase-deficient mice will be valuable animal models to further study the roles of carotenoids in health and disease. FJ

The authors thank Drs. L. T. Webster and M. Maguire for helpful manuscript comments. The authors also thank Catherine Doller (Case Western Reserve University) for performing histological analyses. This work was supported by U.S. National Institute of Health grants EY019641 (to J.V.L.), EY009339, and P30 EY11373, and by a Research to Prevent Blindness grant (to K.P.).

REFERENCES

1. Demmig-Adams, B., and Adams, W. W., 3rd. (2002) Antioxidants in photosynthesis and human nutrition. *Science* **298,** 2149–2153
2. Bernstein, P. S., Yoshida, M. D., Katz, N. B., McClane, R. W., and Gellermann, W. (1998) Raman detection of macular carotenoid pigments in intact human retina. *Invest. Ophthalmol. Vis. Sci.* **39,** 2003–2011
3. Snodderly, D. M., Handelman, G. J., and Adler, A. J. (1991) Distribution of individual macular pigment carotenoids in central retina of macaque and squirrel monkeys. *Invest. Ophthalmol. Vis. Sci.* **32,** 268–279
4. Krinsky, N. I., Landrum, J. T., and Bone, R. A. (2003) Biologic mechanisms of the protective role of lutein and zeaxanthin in the eye. *Annu. Rev. Nutr.* **23,** 171–201
5. Moise, A. R., von Lintig, J., and Palczewski, K. (2005) Related enzymes solve evolutionarily recurrent problems in the metabolism of carotenoids. *Trends Plant Sci.* **10,** 178–186
6. Redmond, T. M., Yu, S., Lee, E., Bok, D., Hamasaki, D., Chen, N., Goletz, P., Ma, J. X., Crouch, R. K., and Pfeifer, K. (1998) Rpe65 is necessary for production of 11-cis-vitamin A in the retinal visual cycle. *Nat. Genet.* **20,** 344–351
7. Von Lintig, J., Kiser, P. D., Golczak, M., and Palczewski, K. (2010) The biochemical and structural basis for trans-to-cis

isomerization of retinoids in the chemistry of vision. *Trends Biochem. Sci.* **35,** 400–410
8. Lindqvist, A., and Andersson, S. (2002) Biochemical properties of purified recombinant human beta-carotene 15,15′-monooxygenase. *J. Biol. Chem.* **277,** 23942–23948
9. Hessel, S., Eichinger, A., Isken, A., Amengual, J., Hunzelmann, S., Hoeller, U., Elste, V., Hunziker, W., Goralczyk, R., Oberhauser, V., von Lintig, J., and Wyss, A. (2007) CMO1 deficiency abolishes vitamin A production from beta-carotene and alters lipid metabolism in mice. *J. Biol. Chem.* **282,** 33553–33561
10. Lindqvist, A., Sharvill, J., Sharvill, D. E., and Andersson, S. (2007) Loss-of-function mutation in carotenoid 15,15′-monooxygenase identified in a patient with hypercarotenemia and hypovitaminosis A. *J. Nutr.* **137,** 2346–2350
11. Kiefer, C., Hessel, S., Lampert, J. M., Vogt, K., Lederer, M. O., Breithaupt, D. E., and von Lintig, J. (2001) Identification and characterization of a mammalian enzyme catalyzing the asymmetric oxidative cleavage of provitamin A. *J. Biol. Chem.* **276,** 14110–14116
12. Hu, K. Q., Liu, C., Ernst, H., Krinsky, N. I., Russell, R. M., and Wang, X. D. (2006) The biochemical characterization of ferret carotene-9′,10′-monooxygenase catalyzing cleavage of carotenoids in vitro and in vivo. *J. Biol. Chem.* **281,** 19327–19338
13. Von Lintig, J. (2010) Colors with functions: elucidating the biochemical and molecular basis of carotenoid metabolism. *Annu. Rev. Nutr.* **30,** 35–56
14. Eriksson, J., Larson, G., Gunnarsson, U., Bed'hom, B., Tixier-Boichard, M., Stromstedt, L., Wright, D., Jungerius, A., Vereijken, A., Randi, E., Jensen, P., and Andersson, L. (2008) Identification of the yellow skin gene reveals a hybrid origin of the domestic chicken. *PLoS Genet.* **4,** e1000010
15. Tian, R., Pitchford, W. S., Morris, C. A., Cullen, N. G., and Bottema, C. D. (2009) Genetic variation in the beta, beta-carotene-9′, 10′-dioxygenase gene and association with fat colour in bovine adipose tissue and milk. *Anim. Genet.* **41,** 253–259
16. Vage, D. I., and Boman, I. A. A nonsense mutation in the beta-carotene oxygenase 2 (BCO2) gene is tightly associated with accumulation of carotenoids in adipose tissue in sheep (*Ovis aries*). *BMC Genet.* **11,** 10
17. Berry, S. D., Davis, S. R., Beattie, E. M., Thomas, N. L., Burrett, A. K., Ward, H. E., Stanfield, A. M., Biswas, M., Ankersmit-Udy, A. E., Oxley, P. E., Barnett, J. L., Pearson, J. F., van der Does, Y., Macgibbon, A. H., Spelman, R. J., Lehnert, K., and Snell, R. G. (2009) Mutation in bovine beta-carotene oxygenase 2 affects milk color. *Genetics* **182,** 923–926
18. He, M., Cornelis, M. C., Kraft, P., van Dam, R. M., Sun, Q., Laurie, C. C., Mirel, D. B., Chasman, D. I., Ridker, P. M., Hunter, D. J., Hu, F. B., and Qi, L. (2010) Genome-wide association study identifies variants at the IL18-BCO2 locus associated with interleukin-18 levels. *Arterioscler. Thromb. Vasc. Biol.* **30,** 885–890
19. Wang, S. S., Schadt, E. E., Wang, H., Wang, X., Ingram-Drake, L., Shi, W., Drake, T. A., and Lusis, A. J. (2007) Identification of pathways for atherosclerosis in mice: integration of quantitative trait locus analysis and global gene expression data. *Circ. Res.* **101,** e11–e30
20. Oberhauser, V., Voolstra, O., Bangert, A., von Lintig, J., and Vogt, K. (2008) NinaB combines carotenoid oxygenase and retinoid isomerase activity in a single polypeptide. *Proc. Natl. Acad. Sci. U. S. A.* **105,** 19000–19005
21. Lobo, G. P., Hessel, S., Eichinger, A., Noy, N., Moise, A. R., Wyss, A., Palczewski, K., and von Lintig, J. (2010) ISX is a retinoic acid-sensitive gatekeeper that controls intestinal beta,beta-carotene absorption and vitamin A production. *FASEB J.* **24,** 1656–1666
22. Hoppel, C. L., Kerner, J., Turkaly, P., Turkaly, J., and Tandler, B. (1998) The malonyl-CoA-sensitive form of carnitine palmitoyltransferase is not localized exclusively in the outer membrane of rat liver mitochondria. *J. Biol. Chem.* **273,** 23495–23503
23. Taylor, S. W., Fahy, E., Zhang, B., Glenn, G. M., Warnock, D. E., Wiley, S., Murphy, A. N., Gaucher, S. P., Capaldi, R. A., Gibson, B. W., and Ghosh, S. S. (2003) Characterization of the human heart mitochondrial proteome. *Nat. Biotechnol.* **21,** 281–286
24. Bouvier, F., Suire, C., Mutterer, J., and Camara, B. (2003) Oxidative remodeling of chromoplast carotenoids: identification of the carotenoid dioxygenase CsCCD and CsZCD genes involved in *Crocus* secondary metabolite biogenesis. *Plant Cell* **15,** 47–62
25. Wallace, D. C. (1999) Mitochondrial diseases in man and mouse. *Science* **283,** 1482–1488
26. Ma, Q. (2010) Transcriptional responses to oxidative stress: pathological and toxicological implications. *Pharmacol. Ther.* **125,** 376–393
27. Kloer, D. P., Ruch, S., Al-Babili, S., Beyer, P., and Schulz, G. E. (2005) The structure of a retinal-forming carotenoid oxygenase. *Science* **308,** 267–269
28. Kiser, P. D., Golczak, M., Lodowski, D. T., Chance, M. R., and Palczewski, K. (2009) Crystal structure of native RPE65, the retinoid isomerase of the visual cycle. *Proc. Natl. Acad. Sci. U. S. A.* **106,** 17325–17330
29. Bhosale, P., and Bernstein, P. S. (2007) Vertebrate and invertebrate carotenoid-binding proteins. *Arch. Biochem. Biophys.* **458,** 121–127
30. Lindqvist, A., He, Y. G., and Andersson, S. (2005) Cell type-specific expression of beta-carotene 9′,10′-monooxygenase in human tissues. *J. Histochem. Cytochem.* **53,** 1403–1412
31. Hartmann, D., Thurmann, P. A., Spitzer, V., Schalch, W., Manner, B., and Cohn, W. (2004) Plasma kinetics of zeaxanthin and 3′-dehydro-lutein after multiple oral doses of synthetic zeaxanthin. *Am. J. Clin. Nutr.* **79,** 410–417
32. Thurmann, P. A., Schalch, W., Aebischer, J. C., Tenter, U., and Cohn, W. (2005) Plasma kinetics of lutein, zeaxanthin, and 3-dehydro-lutein after multiple oral doses of a lutein supplement. *Am. J. Clin. Nutr.* **82,** 88–97
33. Hantz, H. L., Young, L. F., and Martin, K. R. (2005) Physiologically attainable concentrations of lycopene induce mitochondrial apoptosis in LNCaP human prostate cancer cells. *Exp. Biol. Med. (Maywood)* **230,** 171–179
34. Brunelle, J. K., Bell, E. L., Quesada, N. M., Vercauteren, K., Tiranti, V., Zeviani, M., Scarpulla, R. C., and Chandel, N. S. (2005) Oxygen sensing requires mitochondrial ROS but not oxidative phosphorylation. *Cell. Metab.* **1,** 409–414
35. Kaelin, W. G. (2005) Proline hydroxylation and gene expression. *Annu. Rev. Biochem.* **74,** 115–128
36. Burgering, B. M., and Kops, G. J. (2002) Cell cycle and death control: long live Forkheads. *Trends Biochem. Sci.* **27,** 352–360
37. Mantena, S. K., King, A. L., Andringa, K. K., Eccleston, H. B., and Bailey, S. M. (2008) Mitochondrial dysfunction and oxidative stress in the pathogenesis of alcohol- and obesity-induced fatty liver diseases. *Free Radic. Biol. Med.* **44,** 1259–1272
38. Greenwald, P. (2003) Beta-carotene and lung cancer: a lesson for future chemoprevention investigations? *J. Natl. Cancer Inst.* **95,** E1
39. Paolini, M., Antelli, A., Pozzetti, L., Spetlova, D., Perocco, P., Valgimigli, L., Pedulli, G. F., and Cantelli-Forti, G. (2001) Induction of cytochrome P450 enzymes and over-generation of oxygen radicals in beta-carotene supplemented rats. *Carcinogenesis* **22,** 1483–1495
40. Liu, C., Wang, X. D., Bronson, R. T., Smith, D. E., Krinsky, N. I., and Russell, R. M. (2000) Effects of physiological versus pharmacological beta-carotene supplementation on cell proliferation and histopathological changes in the lungs of cigarette smoke-exposed ferrets. *Carcinogenesis* **21,** 2245–2253
41. Ferrucci, L., Perry, J. R., Matteini, A., Perola, M., Tanaka, T., Silander, K., Rice, N., Melzer, D., Murray, A., Cluett, C., Fried, L. P., Albanes, D., Corsi, A. M., Cherubini, A., Guralnik, J., Bandinelli, S., Singleton, A., Virtamo, J., Walston, J., Semba, R. D., and Frayling, T. M. (2009) Common variation in the beta-carotene 15,15′-monooxygenase 1 gene affects circulating levels of carotenoids: a genome-wide association study. *Am. J. Hum. Genet.* **84,** 123–133
42. Leung, W. C., Hessel, S., Meplan, C., Flint, J., Oberhauser, V., Tourniaire, F., Hesketh, J. E., von Lintig, J., and Lietz, G. (2009) Two common single nucleotide polymorphisms in the gene encoding β-carotene 15,15′-monoxygenase alter β-carotene metabolism in female volunteers. *FASEB J.* **23,** 1041–1053

Received for publication September 24, 2010.
Accepted for publication November 11, 2010.